Hindawi Publishing Corporation
EURASIP Journal on Wireless Communications and Networking
Volume 2008, Article ID 390489, 15 pages
doi:10.1155/2008/390489

Research Article

Distributed Iterative Multiuser Detection through Base Station Cooperation

Shahid Khattak, Wolfgang Rave, and Gerhard Fettweis

Vodafone Chair Mobile Communications Systems, Technische Universität Dresden, 01062 Dresden, Germany

Correspondence should be addressed to Shahid Khattak, khattak@ifn.et.tu-dresden.de

Received 1 August 2007; Revised 18 December 2007; Accepted 13 February 2008

Recommended by Huaiyu Dai

This paper deals with multiuser detection through base station cooperation in an uplink, interference-limited, high frequency reuse scenario. *Distributed iterative detection* (DID) is an interference mitigation technique in which the base stations at different geographical locations exchange detected data iteratively while performing separate detection and decoding of their received data streams. This paper explores possible DID receive strategies and proposes to exchange between base stations only the processed information for their associated mobile terminals. The resulting backhaul traffic is considerably lower than that of existing cooperative multiuser detection strategies. Single-antenna interference cancellation techniques are employed to generate local estimates of the dominant interferers at each base station, which are then combined with their independent received copies from other base stations, resulting in more effective interference suppression. Since hard information bits or quantized log-likelihood ratios (LLRs) are transferred, we investigate the effect of quantization of the LLR values with the objective of further reducing the backhaul traffic. Our findings show that schemes based on nonuniform quantization of the "soft bits" allow for reducing the backhaul to 1–2 exchanged bits/coded bit.

1. INTRODUCTION

An ever growing demand for new broadband multimedia services emphasizes the need for higher spectral efficiency in future wireless systems. A higher-frequency reuse is therefore proposed, resulting in the interference from cochannel users outside the cells to dominate, thereby forming a single most important factor limiting the system performance. This interference coming from outside the cell boundaries is commonly referred to as *other cell interference* (OCI). OCI has been treated in [1], where it was suggested that advanced receiver and transmitter techniques can be employed in the uplink and downlink of a cellular system, respectively. Given that the *mobile terminals* (MTs) are low-cost, low-power independent entities, and are not expected to cooperate to perform transmit or receive beamforming, they are assumed to be as simple as possible with most of the complex processing of a cellular system moved to the *base stations* (BSs).

In this paper, we restrict ourselves to advanced receiver techniques for *uplink* communication. Different advanced receiver techniques, suggested in the literature for the uplink, give tradeoffs between complexity and performance. Optimum *maximum likelihood detection* (MLD) [2, 3] is prohibitively complex for *multiple-input multiple-output* (MIMO) scenarios employing higher-order modulation. Linear receivers [4–7] are simpler, but less effective in decoupling the incoming multiplexed data streams, and offer low spatial diversity for full-rank systems. Iterative receivers [8–10] with soft decision feedback offer the best compromise between complexity and performance, and they have been universally adopted as a strategy of choice.

One principal line of thought to address the OCI problem was initiated by *Wyner* 's treatment of base station cooperation in a simple and analytically tractable model of cellular systems [11]. In this model, cells are arranged in either an infinite linear array or in some two-dimensional pattern, with interference originating only from the immediate neighboring cells (having a common edge). All the processing is performed at a single central point. Subsequent work on the information theoretic capacity of the centralized processing systems concluded that the achievable rate per

user significantly exceeds that of a conventional cellular system [12, 13].

Recently, decentralized detection using the belief propagation algorithm for a simple one-dimensional Wyner model was proposed in [14]. The belief propagation algorithm effectively exchanges the estimates for all signals received at each BS, by alternately exchanging likelihood values and extrinsic information. This idea was extended to 2D cellular systems in [15–17], where the limits compared to MAP decoding were studied, showing the great potential of BS cooperation with decentralized processing (at least for regular situations). Unfortunately, for a star network (commonly used today) interconnecting the BSs, this results in a huge backhaul traffic.

Another approach to convert situations where cochannel users interfere each other with comparably strong signals into an advantage for a high-frequency reuse cellular system was proposed in [18]: different BSs cooperate by sending quantized baseband signals to a single central point for joint detection and decoding. Such a *distributed antenna system* (DAS) not only reduces the aggregate transmitted power, but also results in much improved received SINR [19]. Using appropriate receive strategies, both array and diversity gains are obtained, resulting in a substantial increase in system capacity [20, 21]. The DAS scheme, however, is less attractive for network operators due to the large amount of backhaul it requires and the cooperative scheduling necessary between the adjacent DAS units in order to avoid interference. Here, backhaul is defined as the additional communication link between different cooperating entities. Although the bandwidth of wired links used for backhaul can be very high, they are usually owned by a third party, making it attractive for the cellular system operators to reduce the backhaul in order to minimize operating costs. The influence of limited backhaul on capacity in DAS has been investigated in [22, 23].

Similarly as in the mentioned works, we are interested in asymmetric multiuser detection scenarios. We assume that the resource management of the cellular network can detect (e.g., via signal strength indicators) groups of MTs that are strongly received at several base stations. However, in contrast to [15, 17] and related work, our main interest is not the network wide optimum information exchange, but rather its decentralized implementation. To this end, the concept of *distributed iterative detection* (DID) was introduced in [24, 25]: each base station initially performs single-user detection for the strongest MT, treating the signals received from all other mobile terminals as noise. The information that becomes available at the decoder output is then sent to neighboring BS while mutually receiving data from its own neighbors in order to reconstruct and cancel the interference of its own received signal. Single-user detection is then applied to this interference-reduced signal by applying parallel interference cancellation [26]. Further improvements can be achieved by repeated application of this procedure. The questions we try to answer here are as follows.

(i) How much improvement can we get with respect to conventional single-user detection in different scenarios (varying strength of the user coupling through the channel)?

(ii) Which additional gain is possible if we replace the single-user detection step in the 0th iteration with *single-antenna interference cancellation* (SAIC) which is implemented as *joint maximum likelihood detection* (JMLD) in the symbol detector acting as the receiver frontend?

(iii) What is a reasonable trade off between the amount of information exchange and improvement beyond single-user detection? Or, stated otherwise, what happens under constraints for the maximum available data rate over the backhaul links between base stations and associated finite precision effects due to quantization?

The organization of the remainder of this paper is as follows. Section 2 presents the system model, where the coupling among users/cells and the channel model are described. Section 3 discusses in detail various components of distributed iterative receivers. In Section 4 different decentralized detection strategies are compared. In Section 5 we examine the effect of quantization of reliability information. We compare various quantization strategies in terms of information loss and necessary backhaul traffic. Numerical results are presented in Section 6 before conclusions are drawn.

Notation

Throughout the paper, complex baseband notation is used. Vectors are written in boldface. A set is written in double stroke font such as $\mathbb{I}$ and its cardinality is denoted by $|\mathbb{I}|$. The expected value and the estimates of a quantity such as s are denoted as $E\{s\}$ and $\hat{s}$, respectively. Random variables are written as uppercase letters and their realization with lowercase letters. *A posteriori probabilities* (APPs) will be expressed as log-likelihood ratios (L-values). A superscript denotes the origin (or receiver module), where it is generated. We distinguish L^{d1}, L^{d2}, and L^{ext} which are APPs generated at the detector and the decoder of a given BS or externally to it.

2. TRANSMISSION MODEL

We consider an idealized synchronous single-carrier (narrow band) cellular network in the uplink direction. N is the number of receive antennas and M is the number of transmit antennas corresponding to the number of BSs and cochannel MTs, respectively.

A block of information bits $\mathbf{u}_m$ from user antenna m is encoded and bit-interleaved leading to the sequence $\mathbf{x}_m$ of length K, where $m = 1 \cdots M$. This sequence is divided into groups of q bits each, which are then mapped to a vector of output symbols for user m of size $K_s = K/q$ according to $\mathbf{s}_m = [s_{m,1}, \ldots, s_{m,K_s}] = \text{map}(\mathbf{x}_m)$. Each symbol is randomly drawn from a complex alphabet $\mathbb{A}$ of size $Q = 2^q$ with $E\{s_{m,k}\} = 0$ and $E\{|s_{m,k}|^2\} = \sigma_s^2$ for $m = 1 \cdots M$.

A block of K_s symbol vectors $\mathbf{s}[k] = [s_{1,k}, s_{2,k}, \ldots, s_{M,k}]^T$ (corresponding to one respective codeword) is transmitted synchronously by all M users. At any BS l, a corresponding block of symbols $r_l[k]$ is received, where the index k is related to time or subcarrier indices ($1 \le k \le K_s$):

$$r_l[k] = \mathbf{g}_l[k] \cdot \mathbf{s}[k] + n[k], \quad 1 \le k \le K_s. \tag{1}$$

With n we denote the additive zero mean complex Gaussian noise with variance $\sigma_n^2 = E\{n^2\}$. For ease of notation, we omit the time index k in the following, because the detector operates on each receive symbol r_l separately.

The row vector $\mathbf{g}_l$ is the elementwise product $g_{l,m} = h_{l,m}\sqrt{\rho_{l,m}}$ of weighted channel coefficients $h_{l,m}$ of M cochannels seen at the lth BS. The channel coefficient vector $\mathbf{h}_l$, obtained as the current realization of a channel model (the channel is passive on the average, i.e., $E\{|h_{l,m}|^2\} = 1$), is assumed to be known perfectly. The coupling coefficients $\rho_{l,m}$ reflect different user positions (path losses) with respect to base station l. These will be abstracted in the following by two coupling coefficients ρ_i and ρ_j which characterize the BS interaction with strong and weak interferers.

Equation (1) can therefore be written in terms of the desired signal (denoted with the index d) and weak and strong interferences:

$$\begin{aligned} r_l &= g_{ld}s_d + \sum_{i\in\mathbb{I}_l} g_{li}s_i + \sum_{j\in\overline{\mathbb{I}}_l} g_{lj}s_j + n \\ &= h_{ld}s_d + \underbrace{\sqrt{\rho_i}\sum_{i\in\mathbb{I}_l} h_{li}s_i}_{\text{strong interference}} + \underbrace{\sqrt{\rho_j}\sum_{j\in\overline{\mathbb{I}}_l} h_{lj}s_j}_{\text{weak interference}} + n, \end{aligned} \tag{2}$$

where $\rho_{ld} = 1$. We note that this is of course a variant of the two-dimensional *W yner* model. With $\mathbb{I}_l$ we denote the set of indices of all strongly received interferers at BS l with cardinality $|\mathbb{I}_l| = m_l - 1$, where m_l is total number of strongly received signals at BS l. Additionally, $\overline{\mathbb{I}}_l$ is the complementary set for all weakly received interferers: $|\mathbb{I}_l \cup \overline{\mathbb{I}}_l| = M - 1$.

Note that the received signal-to-noise ratio (SNR) is defined as the ratio of received signal power at the nearest BS and the noise power. Specifically, the SNR at the lth BS can be written as $\text{SNR} = E\{\|h_{ld}s_d\|^2\}/E\{n^2\} = \sigma_s^2/\sigma_n^2$.

The considered synchronous model is admittedly somewhat optimistic and was recently criticized due to the impossibility to compensate different delays to different mobiles (positions) simultaneously [27]. However, the reason to ignore synchronization errors is twofold. First, it allows to study the possible improvement through base station cooperation without other disturbing effects to obtain bounds (the degradation from nonideal synchronization should thereafter be included as a second step). Second, for OFDM transmission or frequency domain equalization that we envisage in order to obtain parallel flat channels enabling separate JMLD on each subcarrier, we argue that it is possible to keep the interference due to timing and frequency synchronization errors at acceptable levels.

Increased delay spreads of more distant MTs have to be handled by an appropriately adjusted guard interval in the cooperating region. Timing differences between mobiles lead to phase shifts in the channel transfer function, which are taken into account with the channel estimate. Concerning frequency offsets due to variations among oscillators and Doppler effects, one has to evaluate the intercarrier interference induced by relative shifts of the subcarrier spectra of different users. Roughly estimating this with the $\text{sinc}^2(f/f_{\text{sub}})$ function of the power spectral density for adjacent subcarriers, the SINRshould still be well above 20 dB, if the frequency offset can be kept at the order of 1% and therefore become negligible with respect to the interference to be cancelled on the same resource (oscillator accuracies of 0.1 ppm considered, e.g., in the LTE standardization translate to around 1% in terms of the subcarrier spacing of 15 kHz). We, however, leave the detailed study of asynchronous transmission for future work.

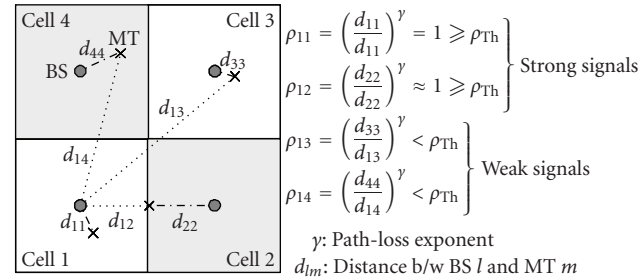

Figure 1: An example setup showing a rectangular grid of 4 cells, with power control assumed with respect to associated BS.

As an example for a cellular scenario that we intend to capture with our model, a rectangular grid of 4 cells is shown in Figure 1, where ρ_{Th} is the path-loss threshold introduced to distinguish between weak and strong interferers. It is defined as the minimum path loss required for an interferer to be detected separately during the BS processing. It depends upon the constellation size and m_l; for example, for 16-QAM and $m_l = 2$ we use $\rho_{\text{Th}} = -12$ dB. Periodic or nonperiodic boundary conditions are possible, allowing for representing extended joint operation or isolated groups of cooperating BSs.

3. DISTRIBUTED ITERATIVE RECEIVER

The setup for performing distributed detection with information exchange between base stations is shown in Figure 2. It comprises one input for the signal r_l generated by the mobile terminals and received at the base station antenna. In addition, it contains a communication interface for exchanging information with the neighboring base stations. This information is either in the form of hard bits $\hat{u}_l$ or likelihood ratios L_l^{d2} of the locally detected signal and corresponding quantities about the estimates of the interfering signals delivered from other base stations. This communication interface is capable of not only transmitting information about the detected data stream to the other base stations, but also receiving information from these base stations.

The receiver processing during initial processing involves either SAIC/JMLD or conventional single-user detection followed by decoding. In subsequent iterations, interference subtraction is performed followed by conventional single-user detection and decoding. Different components of the distributed multiuser receiver are discussed in what follows:

(i) interference cancellation,

(ii) demapping at the symbol detector,

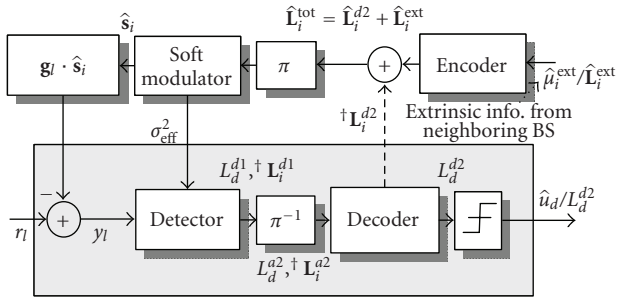

Figure 2: A DID receiver at the lth base station. The subscripts d and i represent the desired data stream and the dominant interferers. Variables designated by † are evaluated only in the first pass of the processing through the receiver. The superscripts 1 and 2 correspond to variables associated with detector and decoder, respectively.

(iii) soft decoding,

(iv) (soft) interference reconstruction.

3.1. Interference canceller and effective noise calculation

At the beginning of every iterative stage, interference of neighboring mobile terminals is subtracted from the signal received at each base station. If r_l is the signal received at the lth base station, the interference-reduced signal y_l at the output of the interference canceller is

$$y_l = r_l - \mathbf{g}_l \cdot \hat{\mathbf{s}}_i = r_l - \sum_{i \in \mathbb{I}_l \cup \bar{\mathbb{I}}_l} g_{li} \hat{s}_i, \tag{3}$$

where $\hat{\mathbf{s}}_i \in \mathbb{C}^{[1 \times n_T]}$ is a vector of symbol estimates. If we exchange only hard decisions about the information bits, then no reliability information is conveyed. Under such condition, additional noise due to the variance of the symbol estimates is not available and the effective noise variance σ_{eff}^2 is underestimated and taken to be equal to that of receiver input noise, that is, $\sigma_{\text{eff}}^2 = \sigma_n^2$. On the other hand, if reliability information for the received bits is available, a vector of error variances $\mathbf{e}_i^2$ for the estimated symbol streams can be calculated. It is then added to the AWGN noise for the subsequent calculations:

$$\sigma_{\text{eff}}^2 = \sigma_n^2 + \sum_{i \in \mathbb{I}_l \cup \bar{\mathbb{I}}_l} |g_{li}|^2 E\{|s_i - \hat{s}_i|^2\} = \sigma_n^2 + \underbrace{\sum_{i \in \mathbb{I}_l \cup \bar{\mathbb{I}}_l} |g_{li}|^2 e_i^2}_{\text{residual-noise}}. \tag{4}$$

The quantities $\mathbf{e}_i^2$ and $\hat{\mathbf{s}}_i^2$ are both evaluated in the soft modulator (see Figure 1) and are discussed in detail in Section 3.4.

Note that if the contributions of weak interferers $\hat{\mathbf{s}}_i \in \bar{\mathbb{I}}_l$ in (4) and (5) are neglected, an error floor will occur in the performance curves, especially at higher-order modulation.

Since both $\mathbf{e}_i^2$ and $\mathbf{s}_i^2$ are evaluated upon arrival of estimates from the neighboring base stations, the interference subtractor is not activated during the first pass and r_l is fed directly into the detector. The effective noise due to inherent interference present in the signal during the first pass is calculated based on the mean transmitted signal power and the number m_d of received signals that are to be jointly detected. Therefore, for the first pass, the effective noise σ_{eff}^2 at the input of the detector of the lth BS, assuming $m_d = m_l$, is given as

$$\sigma_{\text{eff}}^2 = \sigma_n^2 + \sigma_s^2 \sum_{i \in \bar{\mathbb{I}}_l} |g_{li}|^2. \tag{5}$$

3.2. Detection and demapper APP evaluation

The interference-reduced signal y_l and its corresponding noise value are sent to a demapper to compute the a posteriori probability, usually expressed as an L-value [28]. If m_d data streams (each with q bits/sample) are to be detected, the a posteriori probabilities $L^{d1}(x_k|y_l)$ of the coded bits $x_k \in \{\pm 1\}$ for $k = 1 \cdots qm_d$, conditioned on the input signal y_l, are given as

$$L^{d1}(x_k|y_l) = \ln \frac{P[x_k = +1|y_l]}{P[x_k = -1|y_l]}. \tag{6}$$

For $m_d = 1$ single-user detection is applied. When $m_d = m_l$, (where m_l is the number of strong signals at the BS l) JMLD-based single-antenna interference cancellation is applied.

We make the standard assumption that the received bits from any of the m_d data streams in y_l have been encoded and scrambled through an interleaver placed between the encoder and the modulator. Therefore, all bits within y_l can be assumed to be statistically independent of each other. Using Bayes' theorem and exploiting the independence of $x_1, x_2, \ldots, x_{qm_d}$ by splitting up joint probabilities into products, we can write the APPs as

$$\begin{aligned} L^{d1}(x_k|y_l) &= \ln \frac{P(y_l|x_k = +1)P(x_k = +1)}{P(y_l|x_k = -1)P(x_k = -1)} \\ &= \ln \frac{\sum_{\mathbf{x} \in \mathbb{X}_{k,+1}} p(y_l|\mathbf{x}) \prod_{x_i \in \mathbf{x}} P(x_i)}{\sum_{\mathbf{x} \in \mathbb{X}_{k,-1}} p(y_l|\mathbf{x}) \prod_{x_i \in \mathbf{x}} P(x_i)}. \end{aligned} \tag{7}$$

$\mathbb{X}_{k,+1}$ is the set of 2^{qm_d-1} bit vectors $\mathbf{x}$ having $x_k = +1$, and $\mathbb{X}_{k,-1}$ is the complementary set of 2^{qm_d-1} bit vectors $\mathbf{x}$ having $x_k = -1$; that is,

$$\mathbb{X}_{k,+1} = \{\mathbf{x}|x_k = +1\}, \qquad \mathbb{X}_{k,-1} = \{\mathbf{x}|x_k = -1\}. \tag{8}$$

The product terms in (7) are the a priori information about the bits belonging to a certain symbol vector. Since we do not make use of any a priori information in the demapper, these terms cancel out. The L-values at the output of the demapper can now be obtained by taking the natural logarithm of the ratio of likelihood functions $p(y_l|\mathbf{x})$, that is,

$$L^{d1}(x_k|y_l) = \ln \frac{\sum_{\mathbf{x} \in \mathbb{X}_{k,+1}} p(y_l|\mathbf{x})}{\sum_{\mathbf{x} \in \mathbb{X}_{k,-1}} p(y_l|\mathbf{x})}. \tag{9}$$

Calculating likelihood functions

The signal y_l at the detector input contains not only m_d signals that are to be detected at a BS, but also noise and weak interference. For a typical urban environment (assumed here), the number of cochannel interferers from the surrounding cells can be quite large. We therefore make the simplifying assumption that the distribution of the effective noise due to the $(M - m_d)$ interferers together with the receiver noise is Gaussian. The likelihood function $p(y_l|\mathbf{s}_d)$ can then be written as

$$p(y_l|\mathbf{s}_d) = \frac{1}{\pi\sigma_{\text{eff}}^2}\exp\left\{-\frac{1}{\sigma_{\text{eff}}^2}\left(y_l - h_{ld}s_d - \sum_{i\in\mathbb{I}_l} g_{li}s_i\right)^2\right\}, \tag{10}$$

where $\mathbf{s}_d = \text{map}(\mathbf{x})$ is the vector of m_d jointly detected symbols. For single-user detection, $\mathbf{s}_d = s_d$ and the sum term in the exponent of (10) disappears (the subscript "d" in m_d and $\mathbf{s}_d$ denotes the detected streams). This should not be confused with the *desired* user meant by the scalar s_d.

To evaluate (10), the standard trick that we exploit in our numerical simulation is the so-called "Jacobian logarithm":

$$\ln\left(e^{x_1} + e^{x_2}\right) = \max\left(x_1, x_2\right) + \ln\left(1 + e^{-|x_1 - x_2|}\right). \tag{11}$$

The second term in (11) is a correction of the coarse approximation with the max-operation and can be neglected for most cases, leading to the max-log approximation. The APP at the detector output at the lth BS as given in (9) can then be simplified to

$$L^{d1}(x_k|y_l) \cong \max_{\mathbf{x}\in\mathbb{X}_{k,+1}}\left\{-\frac{1}{\sigma_{\text{eff}}^2}\left\|y_l - h_{ld}s_d - \sum_{i\in\mathbb{I}_l} g_{li}s_i\right\|^2\right\} - \max_{\mathbf{x}\in\mathbb{X}_{k,-1}}\left\{-\frac{1}{\sigma_{\text{eff}}^2}\left\|y_l - h_{ld}s_d - \sum_{i\in\mathbb{I}_l} g_{li}s_i\right\|^2\right\}. \tag{12}$$

Despite the max-log simplification, the complexity of calculating $L^{d1}(x_k|y_n)$ is still exponential in the number of the detected bits in $\mathbf{x}$. To find a maximizing hypothesis in (12) for each x_k, there are 2^{qm_d-1} hypotheses to search over in each of the two terms (e.g., 16-QAM modulation with $m_d = 2$ already requires a search over 256 hypotheses to detect a single bit unless other approximations like tree-search techniques [29] are introduced; for lower-order modulation, more than 2 users can certainly be simultaneously detected with acceptable complexity).

3.3. Soft-input soft-output decoder

The detector and decoder in our receiver form a serially concatenated system. The APP vector $\mathbf{L}^{d1}$ (for each detected stream) at the demapper output is sent after deinterleaving as a priori information $\mathbf{L}^{a2}$ to the *maximum a posteriori* (MAP) decoder. The MAP decoder delivers another vector $\mathbf{L}^{d2}$ of APP values about the information as well as the coded bits. The a posteriori L-value of the coded bit x_k, conditioned on $\mathbf{L}^{a2}$, is

$$L^{d2}(x_k|\mathbf{L}^{a2}) = \ln\frac{P[x_k = +1|\mathbf{L}^{a2}]}{P[x_k = -1|\mathbf{L}^{a2}]}. \tag{13}$$

Using the sets $\mathbb{Y}_{k,+1}$ and $\mathbb{Y}_{k,-1}$ to denote all possible codewords $\mathbf{x}$, where bit k equals ± 1, respectively, this can after some mathematical manipulation (see [30]) be simplified to

$$L^{d2}(x_k|\mathbf{L}^{a2}) = \ln\frac{\sum_{\mathbf{x}\in\mathbb{Y}_{k,+1}} e^{(1/2)\mathbf{x}^T\cdot\mathbf{L}^{a2}}}{\sum_{\mathbf{x}\in\mathbb{Y}_{k,-1}} e^{(1/2)\mathbf{x}^T\cdot\mathbf{L}^{a2}}}. \tag{14}$$

3.4. Interference reconstruction

The decoded APP values received from neighboring BS are combined with local information to generate reliable symbol estimates before interference subtraction. It is therefore critical that the dominant interferers are correctly evaluated. Soft symbol vectors $\hat{\mathbf{s}}_i$ estimating the signals of the strongest interferers at BS l are generated from the exchanged extrinsic LLR values $\mathbf{L}_i^{\text{ext}}$ and local dominant interference estimate $\mathbf{L}_i^{d2}$, where $\hat{\mathbf{s}}_i = [\hat{s}_1, \hat{s}_2 \cdots \hat{s}_M]^T$ removing the component of the desired signal with $\hat{s}_d = 0$. Since the channels for the links between one MT and different BSs can be assumed to be uncorrelated, the extrinsic and local LLR values are combined by simply adding them [16], that is,

$$\mathbf{L}_i^{\text{tot}} = \mathbf{L}_i^{\text{ext}} + \mathbf{L}_i^{d2}. \tag{15}$$

The soft symbol estimate $\hat{s}_i$ (one element of the vector $\hat{\mathbf{s}}_i$) is evaluated in the soft modulator [31] by calculating the expectation of the random variable S_i given the combined likelihood ratios associated with the bits of the symbol taken from $\mathbf{L}_i^{\text{tot}}$:

$$\hat{s}_i = E\left\{S_i \,|\, \mathbf{L}_i^{\text{tot}}\right\} = \sum_{s_k\in\mathbb{A}} s_k P\left(S_i = s_k \,|\, \mathbf{L}_i^{\text{tot}}\right), \quad \forall i \in \mathbb{I}_l \cup \overline{\mathbb{I}}_l. \tag{16}$$

The variance of this estimate is equal to the power of the estimation error and it adds to the receiver noise as described in Section 3.1. Any element of the variance vector $\mathbf{e}_i^2 = [e_1^2, e_2^2 \cdots e_M^2]^T$ with $e_d^2 = 0$ is calculated as

$$e_i^2 = \text{var}\left(\hat{s}_i \,|\, L_i^{\text{tot}}\right) = \sum_{s_k\in\mathbb{A}} \left(s_k - \hat{s}_i\right)^2 P\left(S_i = s_k \,|\, L_i^{\text{tot}}\right), \quad \forall i \in \mathbb{I}_l \cup \overline{\mathbb{I}}_l. \tag{17}$$

The error power e_i^2 depends upon the extent of quantization of the LLR values (see Section 5). If only hard bits are transferred, $\hat{s}_i \in \mathbb{A}$ and the estimated symbol error becomes zero, resulting in degraded performance.

4. DECENTRALIZED DETECTION STRATEGIES

The performance of the decentralized processing schemes depends upon receiver complexity and allowable backhaul traffic. In this section, we describe three strategies with increasing complexity that offer different tradeoffs between complexity, performance, and backhaul.

4.1. Basic distributive iterative detection

In the basic version of distributive iterative detection, the decentralized detection problem is treated as parallel interference cancellation by implementing information exchange between the BSs. To keep complexity and backhaul low, only the signal from the associated MT is detected and exchanged between the BSs, while the rest of the received signals are treated as part of the receiver noise. Consider Figure 2, showing the receiver for BS l, where only the desired data s_d is detected with single-user detection and transmitted out to other BSs. The APPs at the output of the soft detector are approximated as

$$L^{d1}(x_k|y_l) \cong \max_{\mathbf{x}\in\mathbb{X}_{k,+1}} \left\{ -\frac{1}{\sigma_{\text{eff}}^2}||y_l - h_{ld}s_d||^2 \right\} - \max_{\mathbf{x}\in\mathbb{X}_{k,-1}} \left\{ -\frac{1}{\sigma_{\text{eff}}^2}||y_l - h_{ld}s_d||^2 \right\}. \tag{18}$$

The decoded estimates of the desired streams are exchanged after quantization. The incoming decoded data streams from the neighboring BS are used to reconstruct the interference energy. Since only the desired data stream is detected, no local estimates of the strongest interferers L_i^{d2} are available, making the symbol estimates less reliable. This scheme needs a higher SIR than the ones presented in Sections 4.2 and 4.3 to converge. It is therefore beneficial only in the case of low-frequency reuse.

4.2. Enhanced distributive iterative detection with SAIC

The performance of the basic distributed detection receiver degrades for asymmetrical channels encountered in high-frequency reuse networks when dominant interferers are present and the SIR $\to$0 dB.

The error propagation encountered in the basic DID scheme is reduced by improving the initial estimate through single-antenna interference cancellation. Although all the detected data streams are decoded, in this approach only the decoded APPs for the desired users are exchanged between the BSs to limit the amount of backhaul. However, the APPs for the dominant interferers are not discarded, but used in conjunction with reliability information from other BSs to cancel the interference. The performance of this scheme is, however, limited by the number of nondetected weak interferers and/or by the quantization of the exchanged reliability information. Therefore, also the number of required exchanges between the BSs to reach convergence is slightly higher than for the unconstrained scheme described next.

Unlike the basic DID scheme, the performance curves for SAIC aided DID to converge even if the SIR is around or below 0 dB (this is similar to the situation in spatial multiplexing with strong coupling among the streams). Since a BS does not receive multiple copies of the desired signal from several neighboring BSs, there is a loss of array gain and spatial diversity for the desired signals.

4.3. DID with unconstrained backhaul

In this version of decentralized detection, all estimates of the received data streams are detected at each BS, and all available soft LLR values are exchanged. This approach uses multiple exchanges of extrinsic information between the BSs and is similar to message passing (although we may use an ML detector during the first information pass). Since all detected input streams are exchanged, both diversity and array gain are obtained. In addition, the algorithm converges more quickly than the ones with constrained backhaul. While the simultaneous detection of multiple data streams through SAIC during initial iteration can further speed up convergence, low-complexity SUD detection during the first iteration is normally sufficient and results in only marginal degradation in performance. The amount of backhaul per iteration for a fully coupled system ($m_l = M$), however, grows cubically in the cooperating setup size, that is, backhaul $\propto MN(M-1)$, making this scheme impractical even for a few BSs in cooperation.

5. QUANTIZATION OF THE RELIABILITY INFORMATION

A posteriori probabilities at the decoder must be quantized before transmission causing quantization noise, which is equivalent to information loss in the system. By increasing the number of quantization levels, this loss will decrease at the cost of added backhaul, which has to stay within guaranteed limits from the network operator's standpoint.

The information content associated with L-values varies with their magnitude. While single-bit quantization will incur little information loss at high reliability values, it leads to considerable degradation in performance for L-values having their mean close to zero. Therefore, L-values following a bimodal Gaussian distribution should not simply be represented using uniform quantization. Even nonuniform quantization according to [32, 33] applied directly to the L-values by minimizing the mean square error (MSE) between the quantized and nonquantized densities is not optimum as we will show. In what follows we develop a quantization strategy based on information-theoretic concepts, such as "soft bits" and mutual information. Representation of the L-values with these quantities takes the saturation of the information content (with increasing magnitude of the L-values) into account and improves the backhaul efficiency.

5.1. Representation of L-values based on mutual information

Mutual information $I(X;L)$ between two variables x and l measures the average reduction in uncertainty about x when l is known and vice versa [34]. We use mutual information to measure the average information loss about binary data if the L-values are quantized. A general expression for mutual information based on entropy and conditional entropy is

$$I(X;L) = H(L) - H(L|X). \tag{19}$$

Assuming equal a priori probability for the binary variable $x \in \{-1, +1\}$, a simplified expression for the mutual information between x and the a posteriori L-value at the decoder output is (in what follows all logarithms are with respect to base 2)

$$I(X;L) = \frac{1}{2}\sum_{x=\pm 1}\int_{-\infty}^{+\infty} p(l|x)\ln\left[\frac{2p(l|x)}{p(l|x=+1)+p(l|x=-1)}\right]dl. \tag{20}$$

Exploiting the symmetry and consistency properties of the L-value density [28], (20) becomes

$$\begin{aligned} I(X;L) &= \int_{-\infty}^{\infty} p(l|x=+1)\left[1-\ln\left(1+e^{-l}\right)\right]dl \\ &= 1 - E\left\{\ln\left(1+e^{-l}\right)\right\}. \end{aligned} \tag{21}$$

If in the last relation the expected bit values or "*soft bits*" [28] defined as $\lambda = E\{x\} = \tanh(l/2)$ are used, then an equivalent expression for the mutual information between X and L is

$$I(X;L) = E\{\ln(1+\lambda)\}. \tag{22}$$

In practice, the expectation in (21) and (22) is approximated by a finite sum over the L-values in a received codeword:

$$I(X;L) \simeq 1 - \frac{1}{K}\sum_{k=1}^{K}\ln\left(1+e^{-l_k x_k}\right) = \frac{1}{K}\sum_{k=1}^{K}\ln\left(1+\lambda_k x_k\right). \tag{23}$$

An expression to calculate the conditional mutual information based solely on the *magnitude* $|l|$ of the APP values was provided in [35]. Consider the entropy $H_b(\mathrm{x})$ of a binary random variable $\mathrm{x} \in \{0, 1\}$ with $\Pr(\mathrm{x}=0) = P$ given by $H_b(x) = -P1\mathrm{d}(P) - (1-P)1\mathrm{d}(1-P)$. If we calculate the binary entropy of the (instantaneous) bit error probability $P_e(l) = e^{-|l|/2}/(e^{|l|/2} + e^{-|l|/2})$, the probability that hard decisions based on the L-values lead to the wrong sign, $l_k x_k = -1$, is given by $\int_0^\infty p(|l|)P_e(l)d|l|$. Now the mutual information between X and L can be compactly written (as the expectation of the complement of the binary entropy of the bit error rate P_e [36]):

$$\begin{aligned} I(X;L) &= 1 - E\{H_b(P_e)\} \\ &= 1 + E\{P_e\ln(P_e) + (1-P_e)\ln(1-P_e)\}. \end{aligned} \tag{24}$$

From the above expressions, three different L-value representations are conceivable for quantization. They are sketched as a function of the magnitude of the L-values in Figure 3:

(i) original L-values,

(ii) soft bits: $\lambda(l) = \tanh(l/2)$,

(iii) mutual information: $I(l) = 1 - H_b(P_e)$.

The underlying L-value density depends only on a single parameter σ_L, because mean and variance are related by $\mu_L = \sigma_L^2/2$ [37]. This density is given as

$$p_L(l) = \frac{1/2}{\sqrt{2\pi}\sigma_L}\left[\exp\left\{-\frac{\left(l-\sigma_L^2/2\right)^2}{2\sigma_L^2}\right\} + \exp\left\{-\frac{\left(l+\sigma_L^2/2\right)^2}{2\sigma_L^2}\right\}\right]. \tag{25}$$

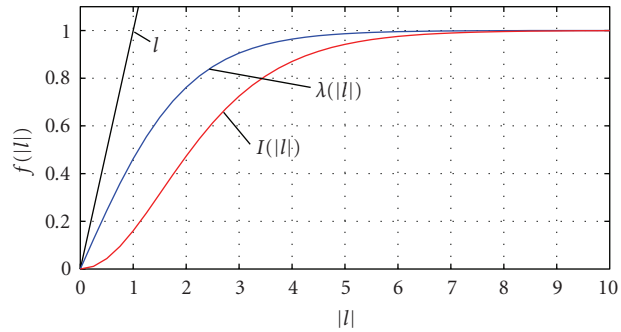

Figure 3: L-value l, soft-bit $\lambda(l)$, and mutual information $I(l)$ representations of the LLR plotted as a function of the magnitude $|l|$ of the LLR.

Using the distribution function (cdf) of $p_L(l)$ and the inverse function $l = 2\tanh^{-1}\lambda$, the transformed soft value density can be obtained in closed form as

$$\begin{aligned} &p_\wedge(\lambda) \\ &= \frac{1/2}{(1-\lambda^2)\sqrt{2\pi}\sigma_L}\left[\exp\left\{-\frac{\left(4\tanh^{-1}\lambda-\sigma_L^2\right)^2}{8\sigma_L^2}\right\}\right. \\ &\qquad \left. + \exp\left\{-\frac{\left(4\tanh^{-1}\lambda+\sigma_L^2\right)^2}{8\sigma_L^2}\right\}\right], \end{aligned} \tag{26}$$

while a mutual information density based on (23) can only be calculated numerically. The three densities that can be alternatively quantized are illustrated in Figure 4. The mutual information density is mirrored at the ordinate to conserve the sign as in the LLR or λ-representations. The performance of different quantization schemes will be investigated next.

5.2. Quantization strategies

Mutual information evaluated with $H_b(P_e)$ and similarly the soft-bit representation are nonlinear functions of L-values that saturate with increasing magnitude. This suggests that nonuniform quantization schemes that minimize the mean-squared quantization error should be able to exploit this and have in addition an advantage over uniform quantization. We adopted the well-known *Lloyd-Max* quantizer to verify our hypotheses.

Nonuniform quantization in the LLR domain

The optimal quantization scheme due to *Lloyd* [32] and *Max* [33] was applied to the L-value density of the decoder output. The *reconstruction* levels r_i are determined through an iterative process after the initial *decision* levels d_i have been set. The objective function to calculate the optimal r_i reads

$$\min_{r_i}\sum_{i=1}^{R}\int_{d_i}^{d_{i+1}}(l-r_i)^2 p(l)dl. \tag{27}$$

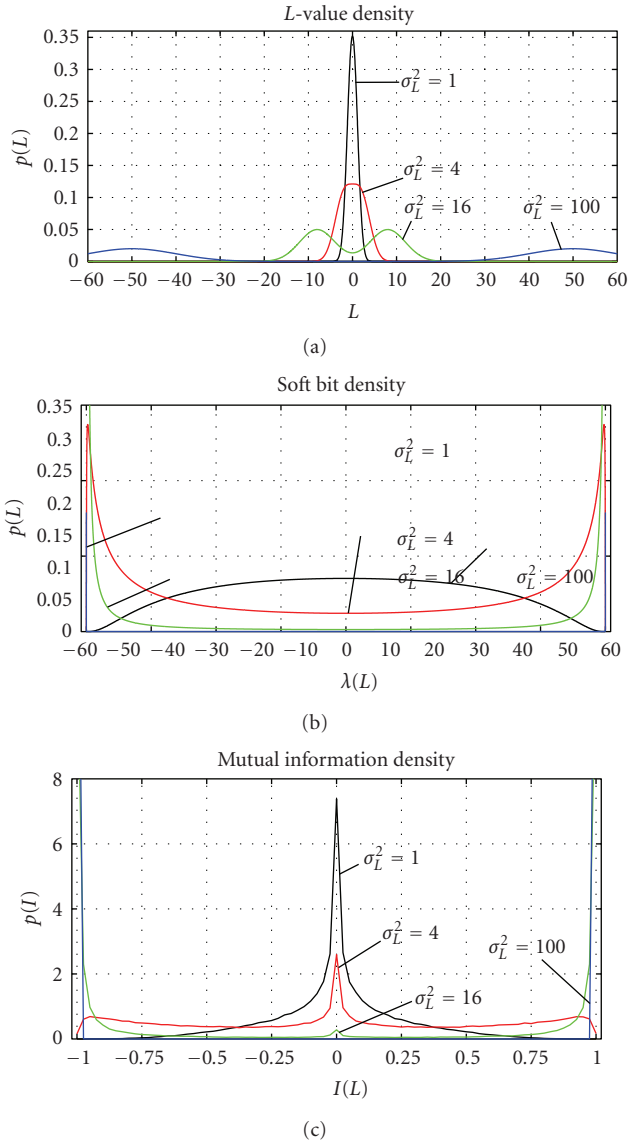

FIGURE 4: Comparison of the distribution of L-values represented in the original bimodal Gaussian form (a) or by soft bits (b) or mutual information (c).

This is iteratively solved by determining the centroids r_i of the area of $p(l)$ between the current pairs of decision levels d_i and d_{i+1}:

$$r_i = \frac{\int_{d_i}^{d_{i+1}} l p(l) dl}{\int_{d_i}^{d_{i+1}} p(l) dl}, \tag{28}$$

and later updating the decision level for the next iteration as

$$d_i = \frac{1}{2}(r_{i-1} + r_i). \tag{29}$$

The number of quantization levels and the number of quantization bits are denoted with $R = 2^b$ and b, respectively. Results for $b = 1, 2$ and 3 bits can be found in the appendix.

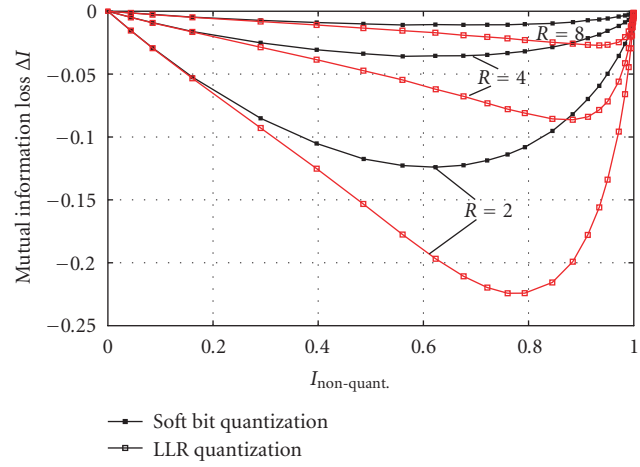

FIGURE 5: Mutual information loss $\Delta I(X;L)$ for nonuniform quantization levels determined in the LLR and soft-bit domains (1–3 quantization bits).

Nonuniform quantization in the soft-bit domain

In this approach, the optimum reconstruction and decision levels to quantize the L-values were calculated in the "soft-bit domain" again in accordance with (27)-(29). Detailed results for $b = 1 - 3$ quantization bits are shown again in the appendix. It should be stressed that the final quantization still occurs in the L-value domain, because the optimized levels are mapped back via $l = 2\tanh^{-1}(\lambda)$. Note that only the number of quantization levels and the variance of the L-values have to be communicated between the BSs to interpret the exchanged data, because the optimized levels can be stored in lookup tables throughout the network.

Mutual information loss

Based on the set of levels d_i and r_i, the mutual information for quantized and nonquantized L-value densities was calculated. The difference represents the reduction or *loss* in mutual information ΔI due to quantization:

$$\Delta I = I_{\text{non-quant}} - I_{\text{quant}}. \tag{30}$$

This loss is shown in Figure 5 as a function of the average mutual information of the nonquantized L-values.

$I_{\text{non-quant}}$ was found with $p_L(l|x = +1)$ evaluating (21). Using the optimized reconstruction and decision levels from the appendix, I_{quant} was determined explicitly as

$$\begin{aligned} I_{\text{quant}} &= \sum_{i=1}^{R} \left[1 - \ln\left(1 + e^{-r_i}\right)\right] \int_{d_i}^{d_{i+1}} p(l|x = +1) dl \\ &= \frac{1}{2} \sum_{i=1}^{R} \left[1 - \ln\left(1 + e^{-r_i}\right)\right] \operatorname{erf}\left(\frac{l - \mu_L}{\sqrt{2}\sigma_L}\right) \Bigg|_{d_i}^{d_{i+1}}. \end{aligned} \tag{31}$$

The larger loss due to quantization of the L-values is clearly visible in Figure 5, where ΔI is plotted for 1-3 quantization bits ($R = 2, 4, 8$ levels).

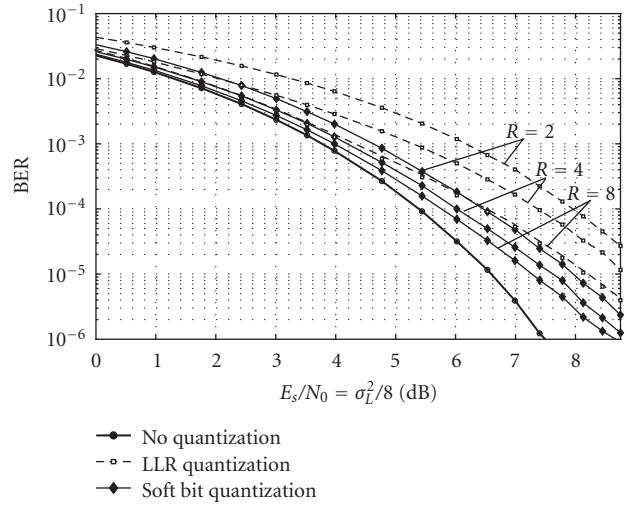

Figure 6: BER after soft combining of L-values for quantized information exchange with optimized levels in either the soft-bit or LLR domain.

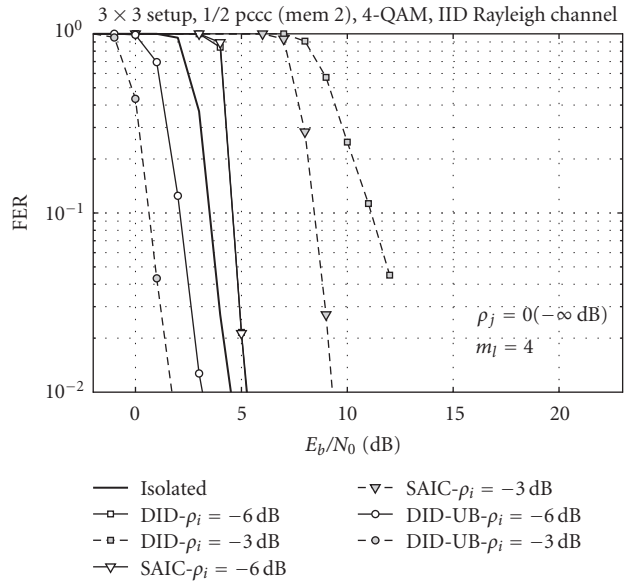

Figure 7: FER curves for different receive strategies in decentralized detection: distributed iterative detection (DID), SAIC-aided DID (SAIC), DID with unconstrained backhaul (DID-UB).

We also tested the combining of two mutual information values with and without quantization as it occurs in decentralized detection with limited backhaul. For transmission of BPSK symbols over an AWGN channel, the relation between SNR and the associated variance of the L-value at the channel output is given by $E_s/N_0 = \sigma_L^2/8$ [36]. Generating two independent distributions for the same σ_L^2 and combining the unquantized L_1 with L_2 according to $L_{\text{tot}} = L_1 + L_2$, we compared the bit error rates (probability of the L-value having the wrong sign) for unquantized L_2 and quantized L_2 based either on optimized quantization levels in the LLR or in the soft-bit domain. Figure 6 shows the BER again for b =1– 3 quantization bits.

We note that the curves for quantization based on the soft-bit domain already for only 1 quantization bit approach the performance of 2 to 3 quantization bits based on the L-value domain.

6. NUMERICAL RESULTS

In this section, we provide simulation results to illustrate the performance of distributed iterative strategies in an uplink cellular system. A synchronous cellular setup of 3×3 cells ($N = M = 9$) or 2×2 cells ($N = M = 4$) is assumed. The number of strongly received signals m_l varies from 1 to 5. The dominant interferers for any BS l are defined by the index set

$$\mathbb{I}_l = \{i : l(\text{mod}\, M) + 1 \le i \le l + m_l(\text{mod}\, M) + 1\}, \quad (32)$$

where $1 \le l \le M$ and $x(\text{mod}\, y)$ represents the modulo operation. As an example, the 2×2 setup with $m_l = 2$ strong interferers and $\rho_j = 0$ is characterized by the following coupling matrix:

$$\rho = \begin{bmatrix} 1 & \rho_i & \rho_i & 0 \\ 0 & 1 & \rho_i & \rho_i \\ \rho_i & 0 & 1 & \rho_i \\ \rho_i & \rho_i & 0 & 1 \end{bmatrix}. \quad (33)$$

The number of symbols in each block (codeword) is fixed to 504. A narrowband flat fading i.i.d. Rayleigh channel model is assumed with an independent channel for each symbol. It is further assumed that the receiver has perfect channel knowledge for the desired user signal as well as the interfering signals. A half-rate memory two-parallel concatenated convolutional code with generator polynomials $(7, 5)_8$ is used in all simulations with either 4-QAM or 16-QAM modulation. The number of information exchanges between neighboring base stations is fixed to five unless otherwise stated.

6.1. Comparison of different decentralized detection schemes

The performance of different decentralized detection schemes described in Section 4 is presented in Figure 7 for a 3×3 setup and 4-QAM modulation.

Three dominant interferers are received at each BS, that is, $m_l = 4$, with normalized dominant interferer path loss $\rho_i \in \{0.25 \quad 0.5\}$ (-3 and -6 dB, resp.). The path loss for the weak interferers ρ_j is assumed to be zero, and unquantized L-values are exchanged. As already mentioned, both basic DID and DID with SAIC have the inherent disadvantage that they only utilize the desired user energy received at the associated BS for signal detection. As a consequence, they do not benefit from array gain or additional spatial diversity and are bounded by the isolated user performance. Although the performance of the basic-DID scheme is comparable to that of SAIC-DID for low values of ρ_i, the difference becomes substantial for higher values of ρ_i. In fact, for $\rho_i \approx 1$ and

for higher-order modulation (16-QAM or higher), the basic-DID scheme does not converge.

In terms of performance, the strategy of exchanging all processed information between the BSs with unlimited backhaul (DID-UB) is the clear winner. This advantage, however, comes at the cost of huge backhaul, with an increase in the number of exchanges between the BSs per iteration $\propto m_l$. Besides, the large array gain of the near-optimal scheme diminishes (not shown here) for less-robust higher-order modulation, that is, 16-QAM.

Figure 8 shows the FER curves for the (3×3) cell setup with $m_l = 4$, $\rho_j = 0$, while the normalized path losses ρ_i of the dominant interferers vary from 0 to 1. Physically, this can be interpreted as an interferer moving away from its own BS towards the base station where the observations are being made. For a network with more than a single tier of neighbors, it is physically impossible to have a high normalized path loss between all the communicating entities. The curve for $\rho_i = 0$ dB is practically not possible and serves only as the indication of the lower performance limits of the receiver. The results for 4-QAM modulation show that the performance stays quite close to an isolated user performance, and has a loss of less than 1 dB at FER of 10^{-2} for $\rho_i \leq -6$ dB.

To show the behavior of a setup with random path losses, the elements ρ_{li} of the path-loss vector are randomly generated with uniform distribution at every channel realization, where $i \in \mathbb{I}_l$ and $0 \leq \rho_i \leq 1$. The simulation results are shown by the dashed curve labeled as "random", which is comparable to $\rho_i = -6$ dB curve.

Figure 9 illustrates the iterative behavior of the SAIC-based receive strategy. There is a large improvement in performance after the initial exchange of decoder APPs, which diminishes with later iterations. We therefore restrict all subsequent simulations to five iterations as very little performance improvement is gained beyond this point.

Figure 10 shows the FER for SAIC-DID plotted as a function of the number of dominant cochannel signals m_l at SNR $= 5$ dB. The FER curve for $\rho_i = -10$ dB indicates that the performance is relatively independent of m_l at low interference levels. However, when $\rho_i \to 1$, the performance degrades considerably with additional interferers. For example, for $m_l = 5$ and $\rho > -6$ dB, the SAIC-DID schemes only start converging at an SNR higher than 5 dB. For a typical cellular setup using directional BS antennas with down-tilt, m_l normally stays between 2 and 4 for 4-QAM, resulting in the FER water fall to be located around 5 dB.

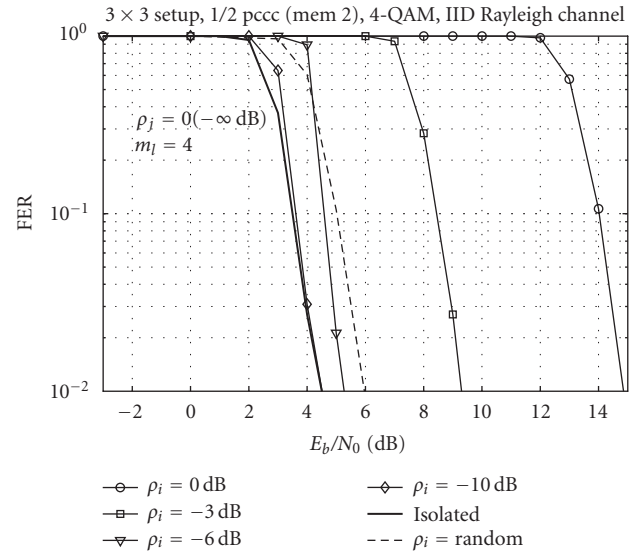

Figure 8: Effect of path loss of the dominant interferer ρ_i, SAIC-DID. For the dashed curve labeled as "random", each element of the path-loss vector $0 \leq \rho_{l,m} \leq 1$, $l \neq m$, is randomly generated with uniform distribution.

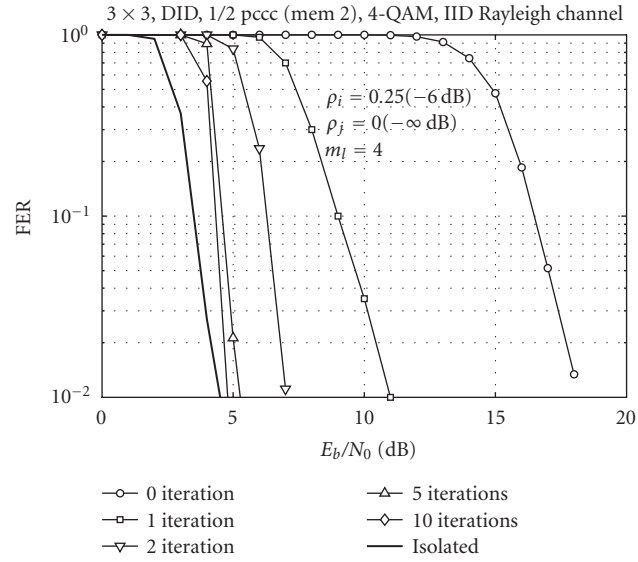

Figure 9: Iterative behavior of SAIC-DID exchanging soft APP values.

6.2. SAIC-DID with unquantized LLR exchange

To see how the performance of a receive strategy scales with the size of the network, Figure 11 depicts a 2×2 cell network in comparison to a 3×3 cell network for different values of the normalized path loss ρ_i. The number of dominant received signals at each BS is fixed to 4. For the solid curves, the set $\mathbb{I}_l$ is defined according to (32), with the modulo operation ensuring that symmetry conditions are incorporated; that is, each MT is received by 4 BSs, while each BS receives 4 MTs. Interestingly, the performance for a 2×2 cell network with greater mutual-coupling is only slightly worse than in a 3×3 cell setup. The mutual-coupling in a 3×3 cell setup can be increased by symmetrically placing the dominant interferers on either side of the leading diagonal. The resulting difference in performance between the setups of two sizes is further reduced (dashed lines). This suggests that for a given number of dominant interferers m_l and coupling ρ_i, the performance depends on the sizes of the cycles that are formed by exchanging information among the BSs.

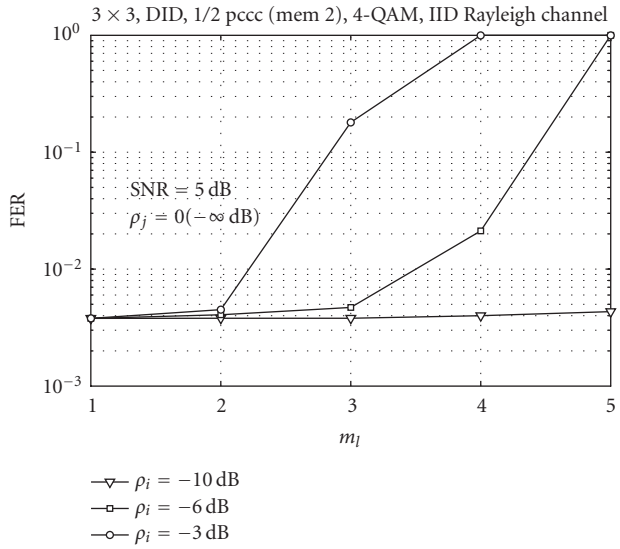

Figure 10: FER for SAIC-DID, plotted as function of the number of dominant cochannel signals m_l at SNR = 5 dB.

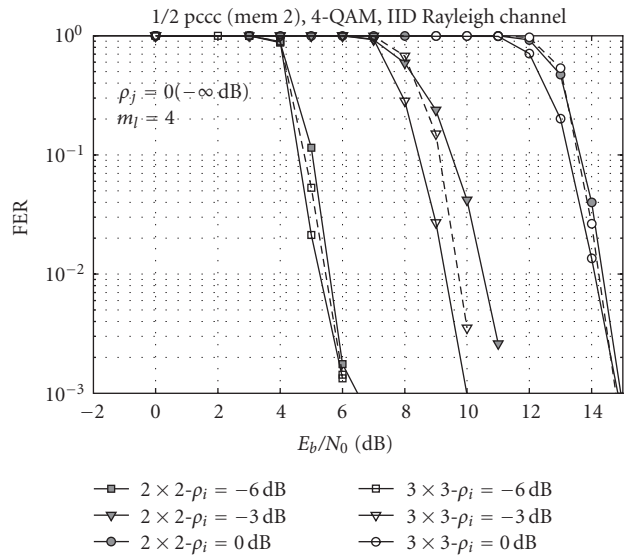

Figure 11: SAIC-DID performance comparison for 2×2 and 3×3 cells setup. Each MT is received strongly at 4 BSs, while each BS receives signals from 4 MTs. The two curves for 3×3 cell setup give the bounds for different possible combinations of couplings within the setup.

Figure 12 shows the performance of SAIC-DID for 4-QAM and 16-QAM modulations, employing a 2×2 cellular setup with only a single dominant interferer, $m_l = 2$, and varying the coupling strength. While the performance of 4-QAM degrades only marginally for $\rho_i = 0$ dB at the FER of 10^{-2}, the loss of the performance for 16-QAM is already more than 3 dB. This indicates that with additional impairments, strong cochannel interferers are difficult to handle for 16-QAM modulation.

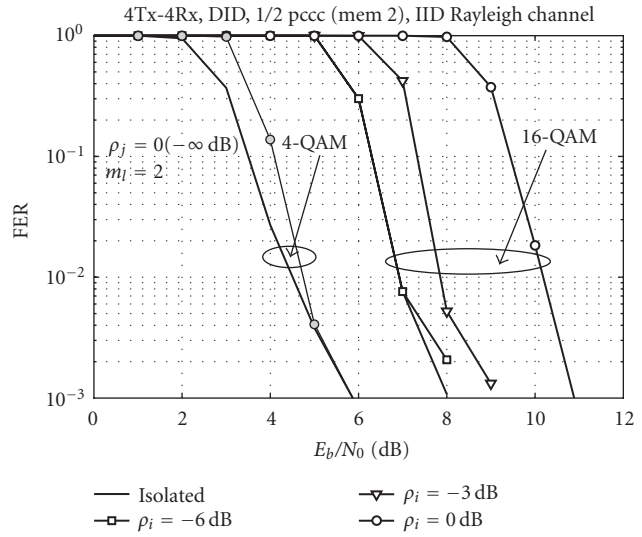

Figure 12: Effect of path loss of the dominant interferer ρ_i for different modulation orders. Each BS sees just two dominant signals $m_l = 2$.

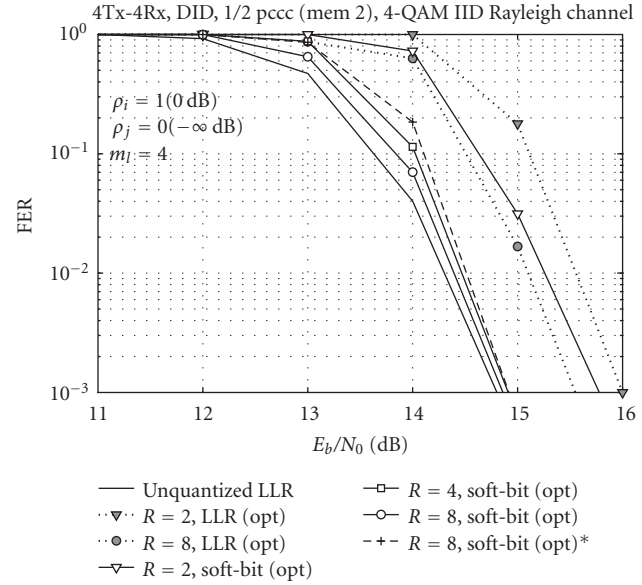

Figure 13: Effect of quantization of the exchanged decoder LLR values, where $\rho_i = 0$ dB. Curve labeled with "+" exchanges only those bits that have changed signs between iterations, and adaptively sets the number of quantization intervals during each iteration to reduce backhaul.

6.3. Quantization of L-values and backhaul traffic

The performance of the proposed scheme for the two different quantization strategies, optimal quantization in the soft-bit and LLR domains, and for different numbers of quantization bits is presented in Figure 13. The normalized path loss $\rho_i = 1$ (0 dB) is chosen such that any loss of quality of the estimates has a pronounced effect on system performance. As already predicted, quantization in the soft-bit domain is clearly superior to that in the LLR domain. For soft-bit domain quantization, exchanging hard bits will

result in a performance loss of one dB which is reduced to almost one quarter of a dB for 2-bit quantization ($R = 4$). Any further increase in quantization bits will bring limited gains.

For the dashed curve labeled with a plus sign ("+") only those bits that have changed signs between iterations are exchanged, and the number of quantization intervals R is set adaptively during each iteration to save backhaul capacity. The maximum number of reconstruction levels is $R_{\max} = 8$. It is illustrated that despite a large improvement in backhaul, the performance degrades only marginally.

As already mentioned, all decoded information bits are only exchanged during the first iteration to minimize the backhaul, while in the later iterations only those bits that have changed signs are exchanged after applying some lossless compression, for example, run-length encoding [38] or vector quantization techniques [39]. Figure 14 shows that the average backhaul traffic during different iterations is plotted as a function of SNR for a hard information bit exchange. In the operating region of interest ($E_b/N_0 > 15$ dB), there is negligible traffic after 3 iterations. The total backhaul in this operating region lies between 100% and 150% of the total number of information bits received, which is a substantial gain over DAS backhaul traffic requirement [19]. It must be mentioned that any additional overhead, required for the compression technique (such as run-length) and used for exchanging a fraction of the estimates, was not taken into account.

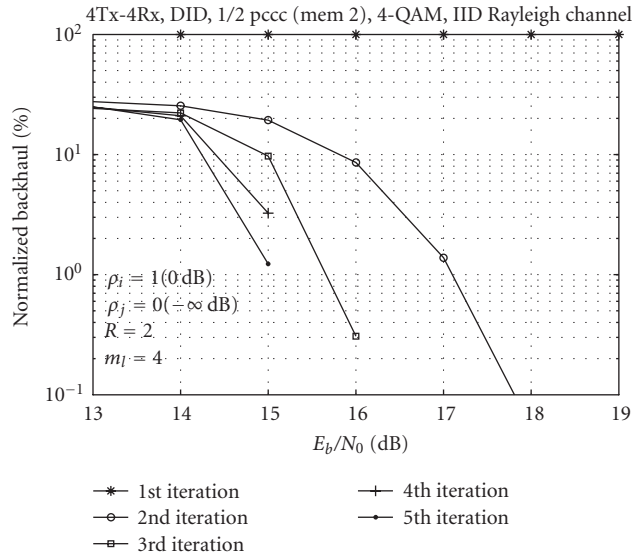

Figure 14: Backhaul traffic normalized with respect to total information bits. Single-bit quantization of LLR values is performed. Only those bits that have changed signs between iterations are exchanged ($\rho_i = 0$ dB).

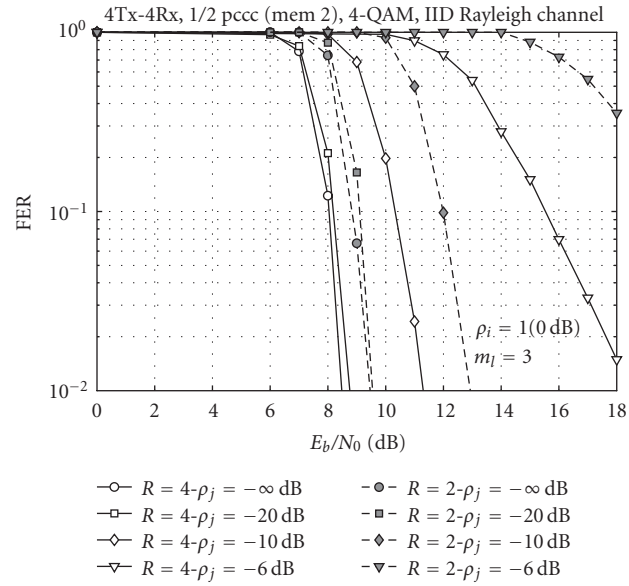

Figure 15: FER for SAIC-DID in the presence of a weak interferer. ρ_j represents the path loss of the weak interferer.

6.4. Sensitivity to additional interference

Finally Figure 15 shows the degradation in the performance of the receiver in the presence of additional weak interferers. As an example, a (2×2) cellular system is considered with three interferers. It is assumed that two interferers are strongly received ($m_l = 3$) with the normalized path loss $\rho_i = 1$ (0 dB), while the third one is a weak interferer whose normalized path loss ρ_j can be varied. As illustrated, the performance deteriorates sharply if $\rho_j > -10$ dB. This is due to the fact that the product constellation of the three stronger streams is quite densely populated and any small additional noise may result in a large change in the demapper output estimates, thereby making the decoder less effective. As to be expected, the schemes become more sensitive to this additional noise after quantization. With comparison to Figure 11 (2×2, 0 dB curve), one can conclude that it is more beneficial for the considered scenario to jointly detect all four incoming signals if the normalized path loss for the weak interferer exceeds -10 dB.

7. CONCLUSIONS AND FUTURE WORK

Outer cell interference in future cellular networks can be suppressed through base station cooperation. We presented an alternative strategy to the distributed antenna system (DAS) for mitigating OCI which we termed as distributed iterative detection (DID). An interesting feature of this approach is the fact that no special centralized processing units is needed. In addition, we explored its implementation with reduced backhaul traffic by performing joint maximum likelihood detection for the desired user and the dominant interferers. We propose to exchange nonuniformly quantized soft bits to minimize the backhaul traffic. Interestingly, the quantization of reliability information does not result in a pronounced performance loss and sometimes even hard bits can be exchanged without undue degradation. To minimize backhaul it is further proposed that only those bits that have changed signs between iterations be exchanged. The result is a considerable reduction in backhaul traffic between base

stations. The scheme is limited by (undetected) background interference.

An extension of this work could address the question under which conditions reliability information for more than one stream should be exchanged to obtain diversity and array gain and when this does not pay. This should provide some further insight into the tradeoff between capacity increase and affordable complexity.

APPENDIX

OPTIMUM QUANTIZATION OF THE L-VALUE DENSITY

To optimize the reconstruction (quantization) levels r_i and decision levels d_i for a given density $p(x)$, we have to iteratively compute the integrals updating the reconstruction levels given the current decision levels d_i (see (29)).

Consider first the bimodal Gaussian density of L-values given in (25). The integrals to be evaluated become (with $\mu_L = \sigma_L^2/2$)

$$\int_{d_i}^{d_{i+1}} \exp\left\{-\frac{(x-\mu_L)^2}{2\sigma_L^2}\right\} + \exp\left\{-\frac{(x+\mu_L)^2}{2\sigma_L^2}\right\} dx = \sigma_L\sqrt{\frac{\pi}{2}}\left[\operatorname{erf}\frac{x-\mu_L}{\sqrt{2}\sigma_L} + \operatorname{erf}\frac{x+\mu_L}{\sqrt{2}\sigma_L}\right]\Bigg|_{d_i}^{d_{i+1}}, \tag{A.1}$$

and

$$\int_{d_i}^{d_{i+1}} x\exp\left\{-\frac{(x-\mu_L)^2}{2\sigma_L^2}\right\} + x\exp\left\{-\frac{(x+\mu_L)^2}{2\sigma_L^2}\right\} dx = \sigma_L^2\left[\exp\left\{-\frac{(x-\mu_L)^2}{2\sigma_L^2}\right\} + \exp\left\{-\frac{(x+\mu_L)^2}{2\sigma_L^2}\right\}\right]\Bigg|_{d_i}^{d_{i+1}} + \mu_L\sigma_L\sqrt{\frac{\pi}{2}}\left[\operatorname{erf}\frac{x-\mu_L}{\sqrt{2}\sigma_L} + \operatorname{erf}\frac{x+\mu_L}{\sqrt{2}\sigma_L}\right]\Bigg|_{d_i}^{d_{i+1}}. \tag{A.2}$$

The optimum positive quantization levels are displayed in Figure 16 (the negative levels are obtained by inversion due to symmetry). As to be expected, for one quantization bit, the level equals the mean more or less exactly. With additional bits, the levels are placed on both sides around the mean. Similar integrals have to be evaluated to quantize nonuniformly in the "soft-bit" domain. Here only one integral can be carried out:

$$\int_{d_i}^{d_{i+1}} p_\wedge(\lambda)d\lambda = \frac{1}{2}\operatorname{erf}\left[\frac{2\tanh^{-1}(\lambda)-\mu_L}{\sqrt{2}\sigma_L}\right]\Bigg|_{d_i}^{d_{i+1}} + \frac{1}{2}\operatorname{erf}\left[\frac{2\tanh^{-1}(\lambda)+\mu_L}{\sqrt{2}\sigma_L}\right]\Bigg|_{d_i}^{d_{i+1}} \tag{A.3}$$

with $p_\wedge(\lambda)$ given by (26). The other integral $\int_{d_i}^{d_{i+1}} \lambda p_\wedge(\lambda)d\lambda$ has to be evaluated by numerical integration. The derived optimum quantization levels converted back to the LLR domain with $L = 2\tanh^{-1}(\lambda)$ are shown in Figure 17.

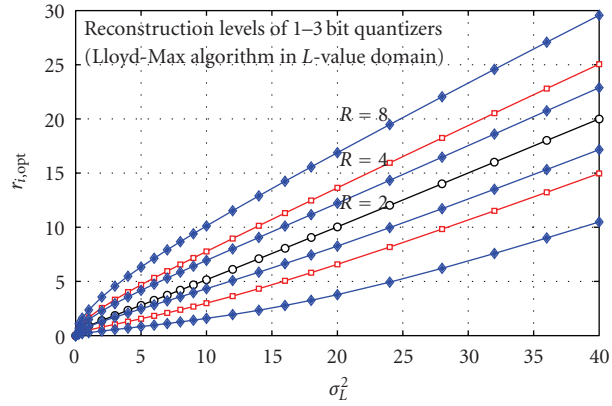

FIGURE 16: Optimum nonuniform quantization levels obtained by optimization in the L-value domain.

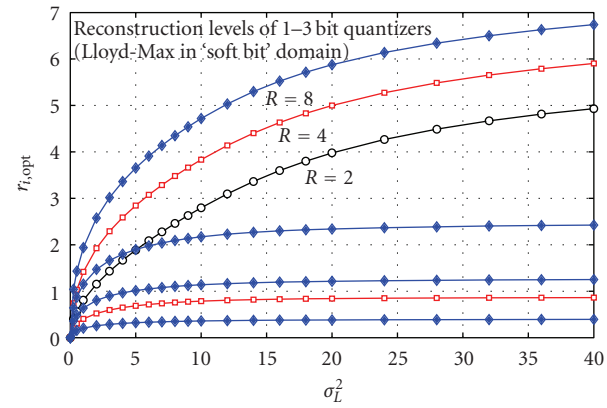

FIGURE 17: Optimum nonuniform quantization levels obtained by optimization in the "soft-bit" domain.

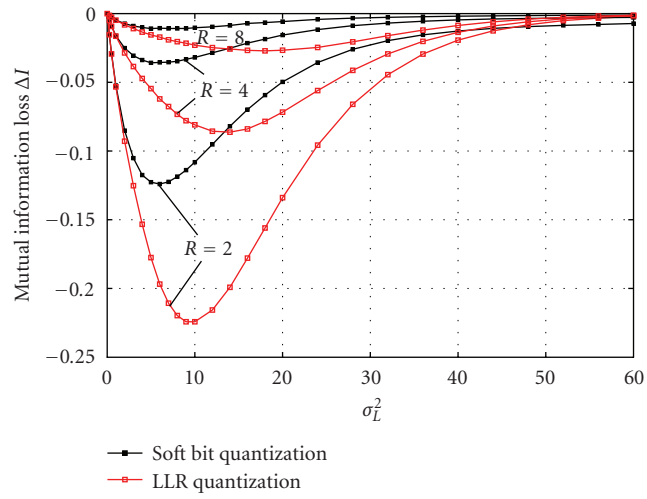

FIGURE 18: Mutual information loss $\Delta I(X;L)$ for 1–3 quantization bits as a function of the variance of the L-values.

We observe that now the optimized levels show some saturation with increasing mean/variance of the L-value density, because the increase in reliability is not important. Rather it pays more to distinguish L-values of intermediate magnitude, say, roughly in the range $2 \leq l \leq 6$.

For practical evaluation, it is more convenient to determine the necessary quantizer resolution according to the variance of the L-values. We therefore provide a plot corresponding to Figure 5 with σ_L^2 as the abscissa in Figure 18.

REFERENCES

[1] J. G. Andrews, "Interference cancellation for cellular systems: a contemporary overview," *IEEE Wireless Communications*, vol. 12, no. 2, pp. 19–29, 2005.

[2] H. Dai, A. F. Molisch, and H. V. Poor, "Downlink capacity of interference-limited MIMO system with joint detection," *IEEE Transactions on Wireless Communications*, vol. 3, no. 2, pp. 442–453, 2004.

[3] J. G. Proakis, *Digital Communication*, McGraw-Hill, New York, NY, USA, 4th edition, 2001.

[4] S. Verdu, "Demodulation in the presence of multiuser interference: progress and misconceptions," in *Intelligent Methods in Signal Processing and Communications*, pp. 15–44, Birkhauser Boston, Cambridge, Mass, USA, 1997.

[5] R. Lupas and S. Verdu, "Linear multiuser detectors for synchronous code-division multiple-access channels," *IEEE Transactions on Information Theory*, vol. 35, no. 1, pp. 123–136, 1989.

[6] U. Madhow and M. L. Honig, "MMSE interference suppression for direct-sequence spread-spectrum CDMA," *IEEE Transactions on Communications*, vol. 42, no. 12, pp. 3178–3188, 1994.

[7] D. Seethaler, G. Matz, and F. Hlawatsch, "An efficient MMSE-based demodulator for MIMO bit-interleaved coded modulation," in *Proceedings of IEEE Global Telecommunications Conference (GLOBECOM '04)*, vol. 4, pp. 2455–2459, Dallas, Tex, USA, November-December 2004.

[8] P. D. Alexander, M. C. Reed, J. A. Asenstorfer, and C. B. Schlegel, "Iterative multiuser interference reduction: turbo CDMA," *IEEE Transactions on Communications*, vol. 47, no. 7, pp. 1008–1014, 1999.

[9] B. Lu and X. Wang, "Iterative receivers for multiuser space-time coding systems," *IEEE Journal on Selected Areas in Communications*, vol. 18, no. 11, pp. 2322–2335, 2000.

[10] H. Lee, B. Lee, and I. Lee, "Iterative detection and decoding with an improved V-BLAST for MIMO-OFDM systems," *IEEE Journal on Selected Areas in Communications*, vol. 24, no. 3, pp. 504–513, 2006.

[11] A. D. Wyner, "Shannon-theoretic approach to a Gaussian cellular multiple-access channel," *IEEE Transactions on Information Theory*, vol. 40, no. 6, pp. 1713–1727, 1994.

[12] S. Shamai and A. D. Wyner, "Information-theoretic considerations for symmetric, cellular, multiple-access fading channels. I," *IEEE Transactions on Information Theory*, vol. 43, no. 6, pp. 1877–1894, 1997.

[13] W. Choi, J. G. Andrews, and C. Yi, "Capacity of multicellular distributed antenna networks," in *Proceedings of the International Conference on Wireless Networks, Communications and Mobile Computing (WIRLES '04)*, vol. 2, pp. 1337–1342, Maui, Hawaii, USA, June 2005.

[14] A. Grant, S. Hanly, J. Evans, and R. Müller, "Distributed decoding for Wyner cellular systems," in *Proceedings 5th Australian Communications Theory Workshop (AusCTW '04)*, pp. 77–81, Newcastle, Australia, February 2004.

[15] E. Aktas, J. Evans, and S. Hanly, "Distributed decoding in a cellular multiple-access channel," in *Proceedings of the IEEE International Symposium on Information Theory (ISIT '04)*, p. 484, Chicago, Ill, USA, June-July 2004.

[16] E. Aktas, J. Evans, and S. Hanly, "Distributed base station processing in the uplink of cellular networks," in *Proceedings of IEEE International Conference on Communications (ICC '06)*, vol. 4, pp. 1641–1646, Istanbul, Turkey, June 2006.

[17] O. Shental, A. J. Weiss, N. Shental, and Y. Weiss, "Generalized belief propagation receiver for near-optimal detection of two-dimensional channels with memory," in *Proceedings of the IEEE Information Theory Workshop (ITW '04)*, pp. 225–229, San Antonio, Tex, USA, October 2004.

[18] A. Sklavos and T. Weber, "Interference suppression in multi-user OFDM systems by antenna diversity and joint detection," in *Proceedings of the COST 273 Management Committee Meeting (MCM '01)*, Bologna, Italy, October 2001, TD(01)020.

[19] S. Khattak, W. Rave, and G. Fettweis, "SIC based multiuser turbo detection in a distributed antenna system for non gray mapping," in *Proceedings of the 9th International Symposium on Wireless Personal Multimedia Communications (WPMC '06)*, San Diego, Calif, USA, September 2006.

[20] W. Roh and A. S. Paulraj, "MIMO channel capacity for the distributed antenna systems," in *Proceedings of the IEEE 56th Vehicular Technology Conference (VTC '02)*, vol. 2, pp. 706–709, Vancouver, BC, Canada, September 2002.

[21] S. Verdu, *Multiuser Detection*, Cambridge University Press, Cambridge, UK, 1998.

[22] P. Marsch and G. Fettweis, "A framework for optimizing the uplink performance of distributed antenna systems under a constrained backhaul," in *Proceedings of the IEEE International Conference on Communications (ICC '07)*, pp. 975–979, Glasgow, Scotland, June 2007.

[23] A. Sanderovich, O. Somekh, and S. Shamai, "Uplink macro diversity with limited backhaul capacity," in *Proceedings of the IEEE International Symposium on Information Theory (ISIT '07)*, Nice, France, June 2007.

[24] S. Khattak and G. Fettweis, "Distributed iterative detection in an interference limited cellular network," in *Proceeding of the 65th IEEE Vehicular Technology Conference (VTC '07)*, pp. 2349–2353, Dublin, Ireland, April 2007.

[25] T. Weber, A. Ahrens, and S. Deng, "Decentralized interference cancellation in mobile radio networks," in *Proceedings of the IEEE Wireless Communications and Networking Conference (WCNC '07)*, pp. 2190–2194, Kowloon, China, March 2007.

[26] V. Kühn, "Combined MMSE-PIC in coded OFDM-CDMA systems," in *Proceedings of Conference IEEE Global Telecommunicatins Conference (GLOBECOM '01)*, vol. 1, pp. 231–235, San Antonio, Tex, USA, November 2001.

[27] H. Zhang, N. B. Mehta, A. F. Molisch, J. Zhange, and H. Dai, "Joint transmission by cooperative base stations in multiuser MIMO cellular downlinks with asynchronous interference," *IEEE Transactions on Wireless Communications*, vol. 7, no. 1, 2008.

[28] J. Hagenauer, E. Offer, and L. Papke, "Iterative decoding of binary block and convolutional codes," *IEEE Transactions on Information Theory*, vol. 42, no. 2, pp. 429–445, 1996.

[29] E. Zimmermann, S. Bittner, and G. Fettweis, "Complexity reduction in iterative MIMO receivers based on EXIT chart analysis," in *Proceedings of the 4th International Symposium on Turbo Codes & Related Topics (ISTC '06)*, München, Germany, April 2006.

[30] B. M. Hochwald and S. ten Brink, "Achieving near-capacity on a multiple-antenna channel," *IEEE Transactions on Communications*, vol. 51, no. 3, pp. 389–399, 2003.
[31] W.-J. Choi, K.-W. Cheong, and J. M. Cioffi, "Iterative soft interference cancellation for multiple antenna systems," in *Proceedings of the IEEE Wireless Communications and Networking Conference (WCNC '00)*, vol. 1, pp. 304–309, Chicago, Ill, USA, September 2000.
[32] S. Lloyd, "Least squares quantization in PCM," *IEEE Transactions on Information Theory*, vol. 28, no. 2, part 1, pp. 129–137, 1982.
[33] J. Max, "Quantizing for minimum distortion," *IEEE Transactions on Information Theory*, vol. 6, no. 1, pp. 7–12, 1960.
[34] T. M. Cover and J. A. Thomas, *Elements of Information Theory*, John Wiley & Sons, New York, NY, USA, 1991.
[35] I. Land, P. A. Hoeher, and S. Gligorevic, "Computation of symbol-wise mutual information in transmission systems with LogAPP decoders and application to Exit charts," in *Proceedings of the 5th International ITG Conference on Source and Channel Coding (SCC '04)*, pp. 195–202, Erlangen, Germany, January 2004.
[36] J. Hagenauer, "The Exit chart," in *Proceedings of the 12th European Signal Processing Conference (EUSIPCO '04)*, pp. 1541–1548, Vienna, Austria, September 2004.
[37] S. ten Brink, "Convergence behavior of iteratively decoded parallel concatenated codes," *IEEE Transactions on Communications*, vol. 49, no. 10, pp. 1727–1737, 2001.
[38] S. Golomb, "Run-length encodings," *IEEE Transactions on Information Theory*, vol. 12, no. 3, pp. 399–401, 1966.
[39] A. Gersho and R. M. Gray, *Vector Quantization and Signal Compression*, Kluwer Academic Publishers, Boston, Mass, USA, 1992.